Diamagnetism and Cooper pairing above T_c in cuprates

Lu Li[1], Yayu Wang[1,2], Seiki Komiya[3], Shimpei Ono[3], Yoichi Ando[3,4], G. D. Gu[5] and N. P. Ong[1]

[1]*Department of Physics, Princeton University, Princeton, NJ 08544*
[2]*Department of Physics, Tsinghua University, Beijing, China*
[3]*Central Research Institute of Electric Power Industry, Komae, Tokyo 201-8511, Japan*
[4]*Institute of Scientific and Industrial Research, Osaka University, Ibaraki, Osaka 567-0047, Japan*
[5]*Brookhaven National Laboratories, Upton, NY 11973*
(Dated: December 16, 2009)

In the cuprate superconductors, Nernst and torque magnetization experiments have provided evidence that the disappearance of the Meissner effect at T_c is caused by the loss of long-range phase coherence, rather than the vanishing of the pair condensate. Here we report a series of torque magnetization measurements on single crystals of La$_{2-x}$Sr$_x$CuO$_4$ (LSCO), Bi$_2$Sr$_{2-y}$La$_y$CuO$_6$ (Bi 2201), Bi$_2$Sr$_2$CaCu$_2$O$_{8+\delta}$ (Bi 2212) and optimal YBa$_2$Cu$_3$O$_7$. Some of the measurements were taken to fields as high as 45 T. Focusing on the magnetization above T_c, we show that the diamagnetic term M_d appears at an onset temperature T_{onset}^M high above T_c. We construct the phase diagram of both LSCO and Bi 2201 and show that T_{onset}^M agrees with the onset temperature of the vortex Nernst signal T_{onset}^ν. Our results provide thermodynamic evidence against a recent proposal that the high-temperature Nernst signal in LSCO arises from a quasiparticle contribution in a charge-ordered state.

PACS numbers: 74.25.Dw, 74.25.Ha, 74.72.Hs

I. INTRODUCTION

A series of experiments utilizing the Nernst Effect [1, 2, 3, 4, 5] has demonstrated that an enhanced Nernst signal is observed in hole-doped cuprates at temperatures T significantly above the superconducting transition temperature T_c. The high-T Nernst region was identified as a continuous extension of the vortex liquid state. In this strongly fluctuating vortex-liquid state, the large Nernst signal arises from phase slippage caused by singular phase fluctuations of the pair condensate [2, 5]. In the phase-disordering scenario, the unbinding of vortex-antivortex pairs (in zero applied H) leads to the loss of long-range phase coherence at T_c [6]. The condensate is incapable of displaying long-range supercurrent response. Hence, even in weak H, there is no Meissner effect above T_c despite the survival of the pair condensate. Nevertheless, the persistent short-range phase stiffness supports vorticity and produces a large, strongly T-dependent Nernst signal in the presence of a temperature gradient $-\nabla T$ and an applied magnetic field $\mathbf{H}$. The Nernst effect above T_c has also been investigated in Refs. [7, 8, 9]

Subsequently, thermodynamic evidence for the pair condensate above T_c was obtained by torque magnetometry, which is a very sensitive probe of diamagnetism in the cuprates [10, 11]. A large diamagnetic response, that is non-linear in H and grows strongly with decreasing T, is specific to the Cooper pair condensate. Consequently, the diamagnetism results present clear evidence for survival of the pair condensate – with sharply reduced phase stiffness – to temperatures high above T_c. This complements the transport evidence from the Nernst experiments. To date, the high-resolution torque measurements above T_c have been reported in the bilayer cuprate Bi$_2$Sr$_2$CaCu$_2$O$_{8+\delta}$ [10, 11, 12, 13, 14] and in lightly-doped La$_{2-x}$Sr$_x$CuO$_4$ at low T [15]. For earlier measurements of diamagnetism above T_c, see Ref. [16] (on Bi 2212) and Ref. [17] (LSCO).

We report further torque magnetization experiments on La$_{2-x}$Sr$_x$CuO$_4$, Bi$_2$Sr$_{2-y}$La$_y$CuO$_6$, Bi$_2$Sr$_2$CaCu$_2$O$_{8+\delta}$ and YBa$_2$Cu$_3$O$_7$, which show that, when a positive Nernst signal appears below the onset temperature T_{onset}, it is accompanied by a large diamagnetic signal that grows steeply with decreasing T. Extending the torque measurements to intense fields (33 T to 45 T), we also show that the curves of M vs. H are nonlinear with a profile characteristic of vortex liquid response, even at elevated T.

Recently, the fluctuating vortex-liquid interpretation of the Nernst effect has been challenged by Cyr-Choiniere *et al.* [18], who carried out Nernst measurements on a series of Nd- and Eu-doped LSCO cuprates, in which charge ordering associated with stripe formation is known to occur at a charge ordering temperature T_{CO}. By a qualitative comparison of the Nernst coefficient ν in Nd-LSCO and Eu-LSCO, Cyr-Choiniere *et al.* proposed that, in pure LSCO, the high-temperature Nernst signal e_N arises from small quasiparticle pockets as a result of Fermi-Surface (FS) rearrangement, rather than from phase-slippage in the pair condensate. We discuss the problem of separating the vortex Nernst term from quasiparticle contributions, and the key role that diamagnetism plays in this task. In pure LSCO, we explain how the magnetization results reported here pose serious difficulties for this hypothesis.

We adopt the abbreviations LSCO 09, LSCO 12 and LSCO 17 for La$_{2-x}$Sr$_x$CuO$_4$ with the Sr content $x = 0.09$, 0.12 and 0.17, respectively. We use Bi 2201 and Bi 2212 to stand for Bi$_2$Sr$_{2-y}$La$_y$CuO$_6$ and Bi$_2$Sr$_2$CaCu$_2$O$_{8+\delta}$, respectively, and YBCO for YBa$_2$Cu$_3$O$_7$. The terms underdoped, optimally-doped and overdoped are abbrevi-

ated as UD, OPT and OV, respectively.

II. TORQUE MAGNETOMETRY

The torque magnetization was measured with the sample glued to the tip of a thin cantilever, with **H** applied at a tilt angle $\theta = 10\text{-}15^{\circ}$ to the crystal c-axis. The deflection φ of the cantilever by the torque was detected capacitively. The cantilever typically can resolve changes in the magnetic moment of $\delta m \sim 10^{-9}$ emu. Because of the 2D electronic dispersion in cuprates, the diamagnetic orbital currents are largely confined to the a-b plane [10, 19]. This makes torque magnetometry well-suited for detecting weak, incipient diamagnetism in cuprate crystals. We generally report the raw data as the effective torque magnetization M_{eff} defined as $M_{eff} = \tau/\mu_0 HV \sin\theta$, where τ is the torque signal, μ_0 the vacuum permeability, and V the sample volume. (M_{eff} includes all contributions to the observed torque signal.)
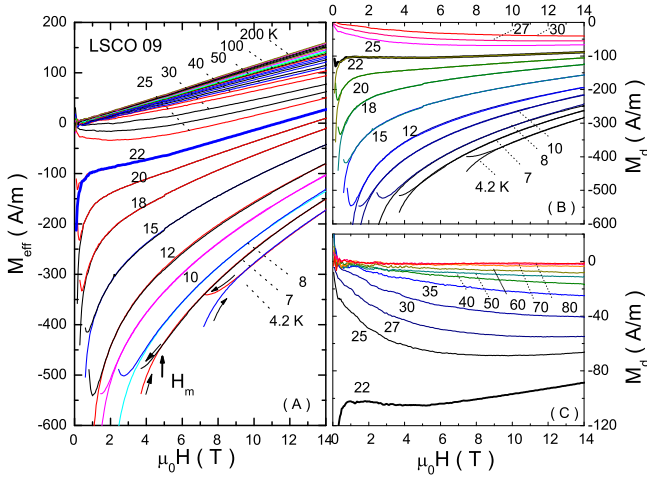

FIG. 1: (color online) Magnetization curves of Sample LSCO 09 with Sr content $x = 0.09$ and transition temperature $T_c = 24$ K measured in magnetic fields H up to 14 T. (A) The (total) effective magnetization M_{eff} vs. H at temperatures $4.2 \leq T \leq 200$ K. Below T_c, the $M_{eff} - H$ curves are hysteretic when H lies below the melting field $H_m(T)$, which is experimentally defined as the field at which the up-sweep branch deviates from the down-sweep branch (H_m is indicated by an arrow for the curve at 7 K). Above H_m, the curves become reversible. (B) The diamagnetic magnetization M_d vs. H at temperatures $4.2 \leq T \leq 30$ K. (C) Curves of M_d vs. H at 22 K $\leq T \leq 80$ K displayed in expanded scale. In LSCO 09, the diamagnetic signal persists to more than 60 K above T_c. In (B) and (C), the bold curve is measured at the separatrix temperature $T_s = 22$ K.

To describe our analysis, we first examine the curves of M_{eff} vs. H shown in Fig.1A for Sample LSCO 09 with $T_c = 24$ K. At temperatures $T > 100$ K, M_{eff} is strictly linear in H and paramagnetic in sign. This reflects the dominance of the anisotropic Van Vleck paramagnetic

susceptibility $\Delta\chi_p$, which has a weak T dependence given by $\Delta\chi_p = A + BT$, with $A \gg BT > 0$ at 200 K. (The T-dependence of M_{eff} will be shown later in Fig. 9.) The reason for measuring a dense set of curves in the high-T interval 100-200 K will emerge when we discuss extraction of the onset temperature for diamagnetic response (Sec. VI). Below 100 K, M_{eff} begins to display a weak diamagnetic contribution that rapidly increases in magnitude as T decreases. The temperature at which the diamagnetic contribution (referred to as M_d hereafter) appears is identified as the onset temperature T_{onset}^M.

We note that M_{eff} becomes increasingly nonlinear in H as T decreases from 60 K to T_c (24 K). Below T_c, the diamagnetic term becomes so dominant in magnitude that M_{eff} is forced to large, negative values despite the positive contribution of the paramagnetic Van Vleck term. At $T < T_c$, the $M_{eff} - H$ curves at low fields display strong hystereses between up-sweep and down-sweep branches because of strong pinning in the vortex-solid state. In the plotted curves, this is seen as a fork (we suppress the full hysteretic curves in both branches for clarity). The field at which the down-sweep branch deviates from the up-sweep branch is experimentally defined as the melting field $H_m(T)$ of the vortex solid (indicated by arrow for the curve at 7 K). As T is raised, H_m decreases rapidly, reaching zero at T_c. A detailed investigation of $H_m(T)$ in lightly doped LSCO is reported in Ref. [15]. The spin contribution to M_{eff}, which becomes important below 2 K in samples with $x < 0.06$, is also treated in detail in Ref. [15].

We assume that the paramagnetic background $\Delta\chi_p H$ follows the trend that is seen at $T > T_{onset}$. Hence the diamagnetic term M_d is related to the observed torque magnetization M_{eff} by

$$M_{eff}(H) = M_d + \Delta\chi_p(T)H = M_d(H) + (A + BT)H. \quad (1)$$

Hereafter, we subtract the background Van Vleck term $(A + BT)H$ from M_{eff} and plot the diamagnetic term M_d vs. H (except stated otherwise).

III. LSCO

Carrying out the background subtraction for LSCO 09, we obtain the M_d vs. H curves. They are displayed at selected T in Fig. 1B (4.2–30 K) and Fig. 1C (20–80 K). As shown in Panel B, M_d is nonlinear in H over a broad temperature interval. The curve at 22 K (bold curve) displays a characteristic flat profile in low fields (0.5 T $< H < 5$ T). We identify this temperature as the "separatrix" temperature T_s [10]. Below T_s, M_d takes on very large, negative values at small H. As H increases, M_d displays an initially steep logarithmic increase, followed by a slower approach towards zero as H approaches the upper critical field H_{c2}. The low-field curvature of the M_d vs. H curve changes from negative below T_s to positive above T_s. To emphasize the high temperature diamagnetic response, panel C displays the $M_d - H$ of Sam-

ple LSCO 09 at $T \geq T_s$ in expanded scale. For $T > T_s$, the curves remain diamagnetic, displaying pronounced nonlinearity vs. H. We regard the nonlinear diamagnetic response above T_c as clear evidence for the presence of local supercurrents as well as finite pair amplitude in the pseudogap state.
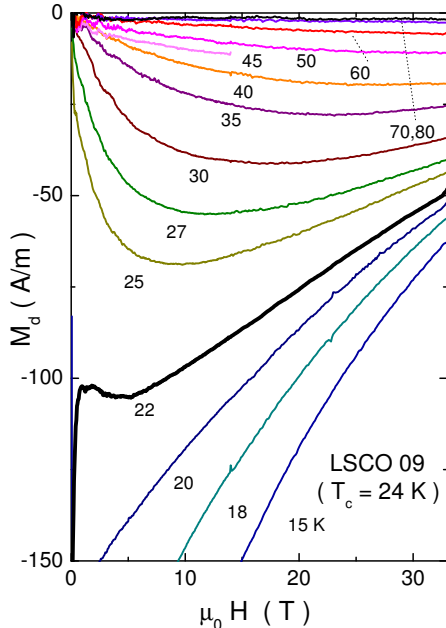

FIG. 2: (color online) Magnetization curves M_d vs. H in LSCO 09 measured in intense fields up to 33 T. T_c lies between the curves at 22 K (bold) and 25 K.
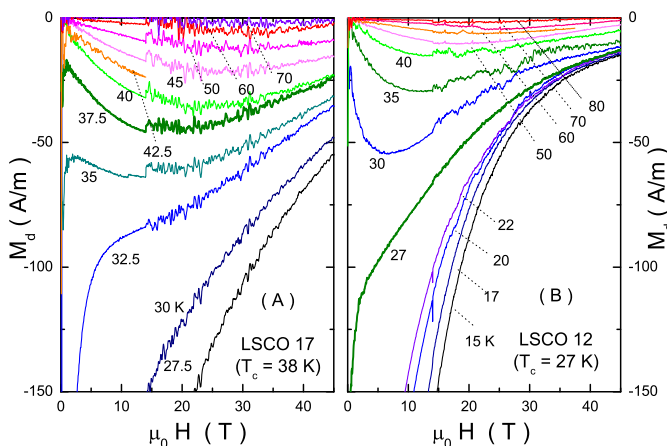

FIG. 3: (color online) Comparison of magnetization curves M_d vs. H in LSC0 17 and LSCO 12 measured in intense fields up to 45 T. Panel A shows curves for Sample LSCO 17 ($x = 0.17$ and $T_c = 38$ K). Panel B displays curves of Sample LSCO 12 ($x = 0.12$ and $T_c = 27$ K).

As in the superconducting state, the diamagnetic signals above T_c can be suppressed by an intense magnetic field. To get a sense of how large this field scale is, we extended the torque measurements on LSCO 09 to 33 T. After the background subtraction described above, the resulting $M_d - H$ curves are isolated and plotted in Fig. 2. For $T > T_c$, these nonlinear $M_d - H$ curves display a broad minimum. The characteristic field H_{min} locating the minimum increases rapidly with T (from 8 T at 25 K to 33 T at 40 K). A rough measure of the field-scale needed to observe the inherent nonlinear response above T_c is given by H_{min}.

We emphasize that, above 50 K, M_d is seemingly linear in H. However, this is simply because H_{min} has now moved outside the experimental window. It is incorrect to attribute – using a limited field range $H < 15$ T – this putative linear behavior to a different mechanism (e.g. quasiparticles with Landau diamagnetism). Above T_c, M_d is inherently non-linear in M up to the onset temperature T_{onset}^M, but one needs progressively higher fields to see the non-linearity as T increases.

The diamagnetic $M_d - H$ curves of Sample LSCO 17 ($x = 0.17$, $T_c = 38$ K) and Sample LSCO 12 ($x = 0.12$, $T_c = 27$ K) measured in H up to 45 T are plotted in Fig. 3A and Fig. 3B, respectively. In these higher-doped crystals, the pattern of the $M_d - H$ curves is broadly similar to that in LSCO 09, and the foregoing discussion applies to the diamagnetic curves. The higher field accessed (45 T) in Fig. 3A, B confirms the intrinsic non-linearity of $M_d(H)$. In Panel A, M_d is manifestly nonlinear at all T up to 70 K, even though it seems linear when the field range is restricted to $H < 10$ T.

The magnitude of M_d in the high-field curves reveals an interesting difference (for $T < T_c$) between LSCO 17 and LSCO 12. The monotonic decrease of $|M_d|$ with H provides an estimate of the upper critical field scale H_{c2} (by extrapolating $M_d \to 0$). Comparing LSCO 17 with LSCO 12, we see that the scale of $|M_d|$ above 20 T is 2-3 times larger in the former at the same H and T. However, the stronger curvature of M_d vs. H in LSCO 12 implies that the decay of M_d is more gradual, so that its H_{c2} is actually higher than that in LSCO 17. In the related cuprate $La_{2-x}Ba_xCuO_4$, stripe formation at $x = \frac{1}{8}$ drives T_c to 4 K [20]. The "dip" in the T_c dome in the phase diagram of LSCO suggests that fluctuating stripes may also exist at $x = \frac{1}{8}$. If this is true, the M_d results suggest that fluctuating stripes reduce the overall pair condensate strength (compared with $x = 0.17$) but allows it to survive to slightly larger fields.

IV. BISMUTH-BASED CUPRATES

The nonlinear diamagnetic signals above T_c are also observed in the single-layer $Bi_2Sr_{2-y}La_yCuO_6$ (Bi 2201) family. In this series, the transition temperature T_c is tuned by the La content y. The optimal T_c occurs at $y \sim 0.44$. Samples with $y > 0.44$ are UD, while those
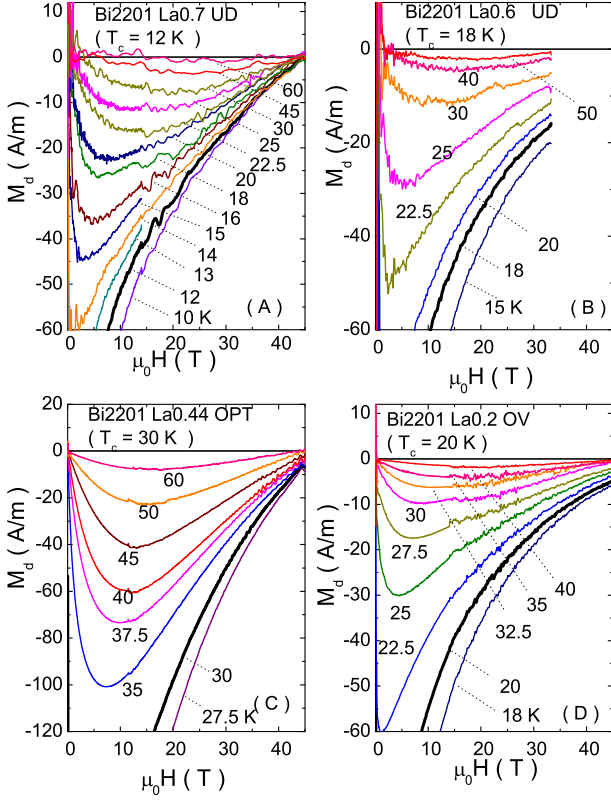
with $y < 0.44$ are OV.

FIG. 4: (color online) Curves of magnetization M_d vs. H in Bi 2201 measured in intense fields. Panel A displays results on UD Sample Bi 2201 (La content $y = 0.7$ and $T_c = 12$ K). Note that most of the results shown are at T above $T_c = 12$ K. They approach zero at the same nominal field scale$\sim$42 T. Panel B plots curves of M_d vs. H measured in another UD Bi 2201 (La content $y = 0.6$ and $T_c = 18$ K). Panels C and D display M_d curves measured in optimally-doped Bi 2201 (La content $y = 0.44$ and $T_c = 30$ K) and OV Bi 2201 (La content $y = 0.2$ and $T_c = 20$ K). In all these Bi 2201 samples, the curves of M_d vs. H remain strikingly nonlinear high above T_c. In each panel, the curve closest to T_c is shown in bold. A preliminary version of Panel A was published in Ref. [12].

Figure 4 displays the diamagnetic $M_d - H$ curves of the single-layer cuprate Bi 2201 samples in the UD region (Panel A and B), in the optimally-doped region (C), and in the OV region (D). Above T_c, the $M_d - H$ curves in Bi 2201 are also similar to those in LSCO shown in Fig. 2 and Fig. 3, except that the magnitudes of M_d and field scales are slightly smaller in the former. Above T_c, M_d attains a broad minimum at fields below 20 T, and then approaches zero at $H \geq 40$ T. Like the curves for LSCO in Fig. 2 and Fig. 3, the curvature of the low-field $M_d - H$ curves changes from negative to positive as T increases across T_c. As H is increased beyond 20
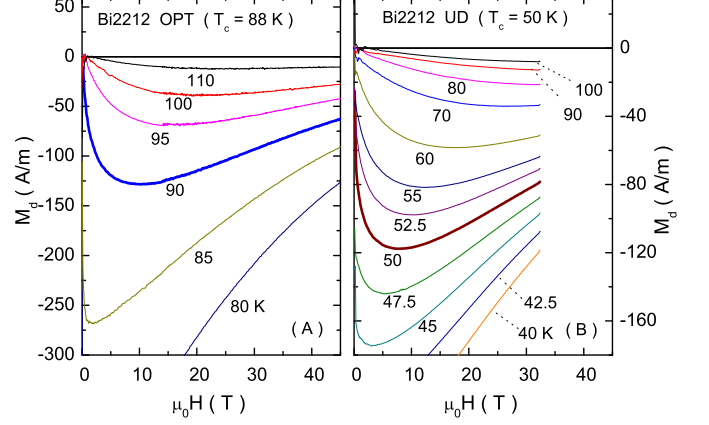

FIG. 5: (color online) Comparison of high-field magnetization curves M_d vs. H in OPT Bi 2212 and UD Bi 2212. Panel A [12] displays the M_d curves in OPT Bi 2212 ($T_c = 88$ K) in fields up to 45 T. Panel B plots magnetization curves in UD Bi 2212 ($T_c = 50$ K) in fields up to 33 T. In each panel, the curve closest to T_c is shown in bold. Panel (A) is taken from Ref. [12].

T, M_d is greatly suppressed. Above T_c, the complete suppression of M_d requires very high fields – comparable to those needed below T_c. Even in UD Bi 2201 with $y = 0.7$, where $T_c =$ is quite low (12 K), the M_d curves are suppressed to zero at $H \sim 38$ - 42 T at $T \leq 45$ K. Above T_{onset}^M (~ 50 K in this sample), M_d vanishes throughout our entire field range. The interesting weak-field region is discussed under "fragile London rigidity".

In Fig. 5, we compare the curves in OPT and UD bilayer Bi 2212 (Panels A and B, respectively). Relative to the single-layer Bi 2201, the amplitude $|M_d|$ in Bi 2212 attains much larger values, and extend to higher field scales. By extrapolating the low-T M_d-H curves, we estimate that H_{c2} exceeds $\sim$150 T (compared with 50-80 T for Bi 2201).

Fragile London Rigidity

One of the most interesting features of the vortex liquid state above T_c is the fragile London rigidity, observable in the limit $H \to 0$. In Ref. [11], Li *et al.* discovered that over a broad interval of T (86-105 K) in OPT Bi 2212, the low-H M_d follows the power-law dependence

$$M_d(T,H) \sim -H^{1/\delta(T)} \quad (H \to 0), \qquad (2)$$

with an exponent $\delta(T)$ that grows rapidly from 1 (at $T \simeq 105$ K) to large values (>6) as $T \to T_c^+$. This implies that the weak-field diamagnetic susceptibility $\chi = \lim_{H \to 0} M/H \to -\infty$ is weakly divergent throughout the interval in T where $\delta > 1$. However, this divergence is extremely sensitive to field suppression. The fragile London rigidity seems to reflect the increasing tendency of the phase-disordered condensate to establish long-range superfluid response as $T \to T_c^+$. It has no ana-

log in bulk samples of low-T_c superconductors, but may exist in a finite T interval above the Kosterlitz-Thouless (KT) transition in 2D systems such as $Mo_{1-x}Ge_x$ and InO_x.

Using a soft cantilever, we have observed a similar pattern of magnetization in OPT Bi 2201. As shown in Fig. 6A, the M_d curves display increasingly strong curvature as H approaches zero from either direction. As T decreases from 38 K to T_c (30 K), the zero-H slope rises sharply to a vertical line (see expanded scale in Panel B). The curve at T_c (bold curve) seems to approach a logarithmic dependence vs. H (equivalent to $\delta \to \infty$). (As may be seen by the oscillations, mechanical noise in this soft cantilever precludes accurate measurements for $|H| < 300$ Oe. In Ref. [11], high-resolution SQUID magnetometry was used to extend measurements down to 10 Oe, but the volume of the present Bi 2201 crystal is too small for similar SQUID measurements.) Despite the lower resolution, the divergent curvature apparent in Fig. 6 is consistent with the appearance of fragile London rigidity starting 8 K above T_c. The curves in Fig. 6B are remarkably similar to those reported in [11, 14] for OPT Bi 2212.

The fragile London rigidity is likely to extend over a larger T interval in UD samples. However, it would be more difficult to disentangle the intrinsic weak-H, non-linear M_d-H behavior from the effects of inhomogeneous broadening arising from local variations of T_c. In OPT samples, we reason that such effects are minimized. The bulk of the sample has the maximum (OPT) T_c. Minority regions with lower T_c contribute only negligibly to the screening current. Hence, observation of the fragile state in OPT samples uncovers, in our opinion, a highly unusual feature of cuprates that is intrinsic.

Contour Plot

An instructive way to view the nonlinear diamagnetic magnetization is the contour plot of M_d in the T-H plane [13]. Figure 7 displays the contour plot in single-layer UD Bi2201 (La content $y = 0.7$, $T_c = 12$ K). The value of $|M_d|$ is as indicated at selected contours. With H fixed (e.g. at 10 T), $|M_d|$ decreases monotonically as T is raised from 4 K to 60 K. Just as in the Nernst signal, the diamagnetic signal in the T-H plane bulges out to temperatures high above T_c, with no obvious discontinuities or changes of slope. The highest temperature at which M_d is resolved is $\sim$50 K (the onset temperature in this sample). The absence of a boundary at T_c implies that the vortex-liquid state below T_c evolves continuously to the diamagnetic state above T_c.

If we fix T (e.g. at 4 K) and increase H, $|M_d|$ also decreases rapidly, as plotted in Fig. 4. The field H_{c2} (=45 T) at which $M_d \to 0$ is plotted as open circles. With increasing T, $H_{c2}(T)$ gradually decreases, roughly tracking the contour at 2 A/m. However, unlike the mean-field BCS scenario, H_{c2} remains very large at T_c (arrow). The magnetization contour plots in Bi 2212 (see Ref. [13]) are roughly similar to that in Fig. 7. However, the scale
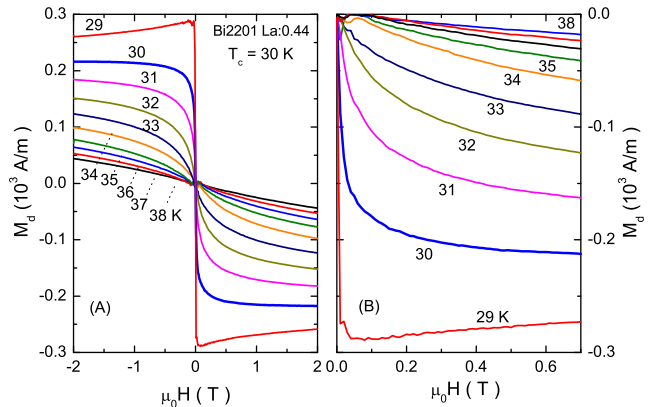

FIG. 6: (color online) The low-field magnetization curves of OPT Bi2201 (La content $y = 0.44$). In Panel (A), the striking weak-field non-linearity is highlighted by displaying the variation of M_d from $H=$ -2 T to +2 T. Although $T_c = 30$ K (bold curve), diamagnetism is observed up to the onset temperature $T_{onset}^M \simeq 70$ K. Panel (B) shows the low-field curvature in expanded scale. The measurements were performed using a very soft cantilever beam. The divergent curvature of M_d at zero H is consistent with fragile London rigidity [11, 14].

of the magnitude $|M_d(T, H)|$ is much larger as expected. $M_d(T, H)$ also extends to much higher field scales. A particular feature is that, near T_c, the contours in OPT Bi 2212 are nearly vertical up to 33 T (the maximum applied field) [13]. This implies that, at the separatrix at T_s, M_d remains nearly H-independent up to 33 T. By contrast, in Bi 2201, the constancy extends only to 10 T, as may be seen in Fig. 7.

V. OPTIMALLY-DOPED YBCO

Optimally-doped YBCO ($T_c= 92$ K) is distinguished as the cuprate with the smallest resistivity anisotropy and the largest interlayer (c-axis) coupling energy. Because the coherence-length anisotropy ξ_a/ξ_c= 3-5 is only moderate, the vortices have the largest stiffness modulus along **c** among cuprates (ξ_a and ξ_c are the coherence lengths along the axes **a** and **c**, respectively). Accordingly, the vortex solid melting line $H_m(T)$ rises very rapidly below T_c (to $\sim$15 T at 87 K). In the vortex-solid state ($H < H_m$), the dissipationless state survives to fields of 60 T or more. Optimally-doped YBCO should be the least susceptible to the phase disordering mechanism for the destruction of long-range phase coherence at T_c (and hence the best candidate for Gaussian fluctuations among cuprates).

However, the torque measurements reveal that T_c in OPT YBCO is also dictated by large phase fluctuations. Figure 8A displays the M_d-H curves in OPT YBCO (twinned) measured to 14 T. The curves are broadly similar to those in LSCO 17 and OPT Bi2212, except for the

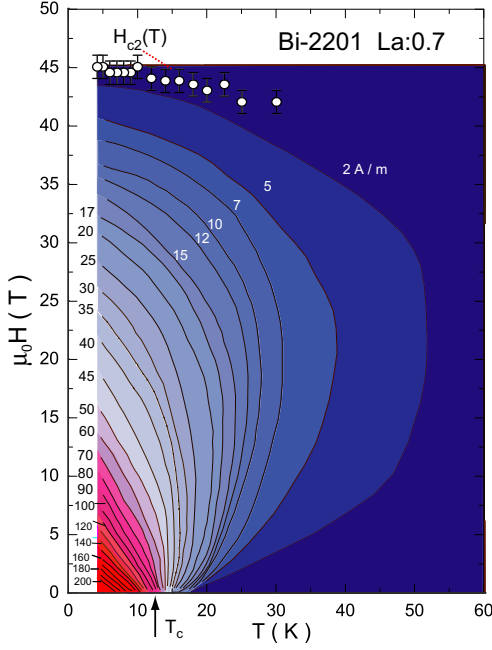FIG. 7: (color online) Contour plot of the diamagnetic magnetization $|M_d(T,H)|$ of UD Bi 2201, with La content $y = 0.7$ and $T_c = 12$ K (arrow). The spacing between adjacent contour lines is 10 A/m for $T < T_c$. The upper critical field H_{c2} (defined by extrapolating $M_d \to 0$) is plotted as open circles.

larger magnitude of $|M_d|$ (at comparable H and T). At $T_c = 92$ K, $|M_d|$ reaches the substantial value ~ 60 A/m at 14 T (by contrast, it should be nearly unobservable in a Gaussian mean-field picture). Over the broad interval $92 \to 130$ K, a large diamagnetic signal is easily observed. As in the other hole-doped cuprates, very intense fields are needed to suppress M_d in this interval.

In Panel (B), we plot the T dependence of the total torque magnetization M_{eff} observed at 14 T (solid circles). As in the other hole-doped cuprates, M_{eff} is unresolved from the Van Vleck line $(A + BT)H$ until T reaches $T_{onset}^M \sim 130$ K (arrow), below which it accelerates to very large negative values. For comparison, we have also plotted the magnetization measured in a very weak $H \sim 10$ Oe (dashed curve) using a SQUID magnetometer. The nearly vertical decrease signals flux expulsion at T_c. We remark that, although M_d – measured with H=10 Oe – is virtually unresolvable above T_c, the diamagnetic susceptibility χ is actually quite large above T_c (as is clear from Panel A). Because M_d is robust to intense H (100 T), the curve at 14 T reveals the existence of the large fluctuating diamagnetism associated with the vortex liquid. This point, emphasized in Refs. [10, 11], highlights the major difference between the diamagnetism in hole-doped cuprates and low-T_c superconductors. In the latter, increasing H in the fluctuation regime above T_c rapidly squelches the (Gaussian) fluctuation signal altogether. The curves in Fig. 8A displaying significant diamagnetism surviving to intense fields,
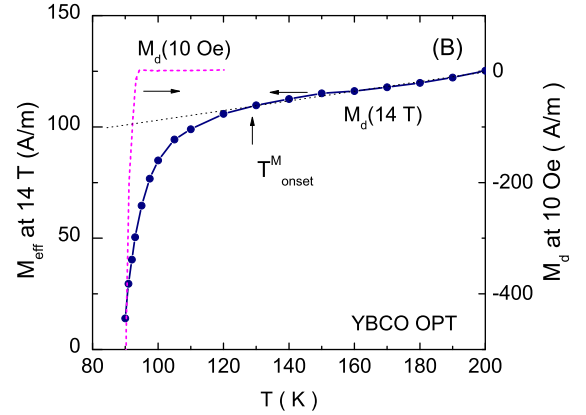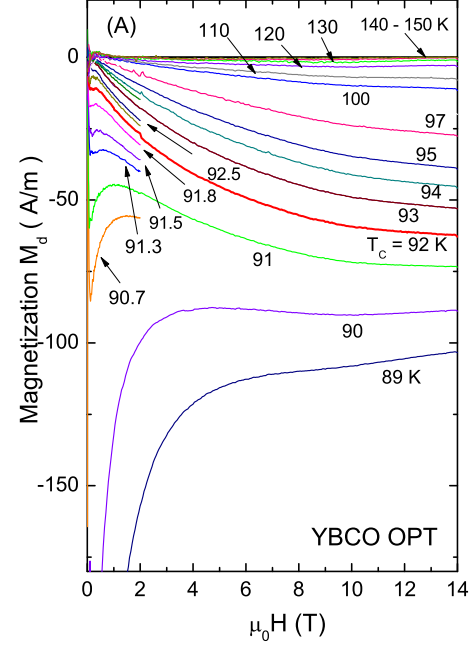

FIG. 8: (color online). Magnetization curves of OPT YBa$_2$Cu$_3$O$_{7-\delta}$. Panel (A) displays curves of M_d vs. H from $T = 89$ to 150 K. Some curves were taken (at slower sweep rate) only to 1 T. Above $T_c = 92$ K (bold curve), a sizeable diamagnetic signal persists to $T_{onset}^M \sim 130$ K. Panel (B) plots the T dependence of the observed M_{eff} with $H = 14$ T. As in the other cuprates, M_{eff} may be fit to a straight line above the onset of the diamagnetic signal T_{onset}^M. The dashed curve is the Meissner signal M_{sq} measured by SQUID magnetometry with H= 10 Oe.

at temperatures up to 40 K *above* T_c is strong evidence that we are observing the phase-disordering mechanism, rather than Gaussian mean-field fluctuations. A comparison of the Nernst and magnetization signals in UD YBCO is given in Ref. [24].

FIG. 10: (color online) Expanded view of the total observed magnetization M_{eff} vs. H in LSCO 09 (Panel A) and LSCO 12 (B). Above T_{onset}^M, the T dependence of the curves is only from the paramagnetic Van Vleck term. Below T_{onset}^M, however, the diamagnetic term M_d grows rapidly to dominate the T dependence. The stability of the torque cantilever and the resolution in τ are sufficient to allow closely spaced curves to be resolved. The uncertainty in measuring M_{eff} makes the largest contribution to the error bars in T_{onset}^M.
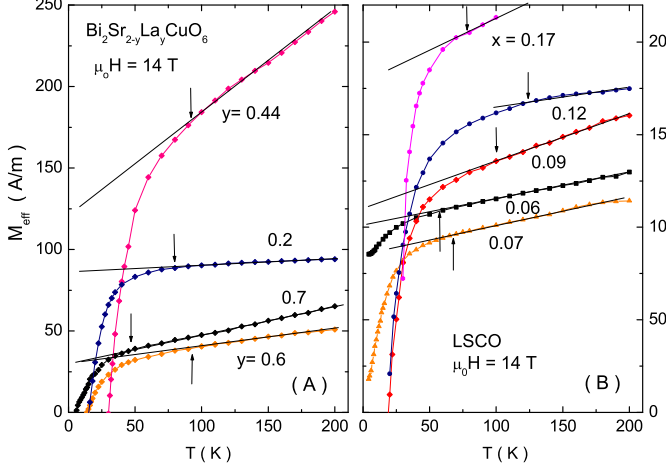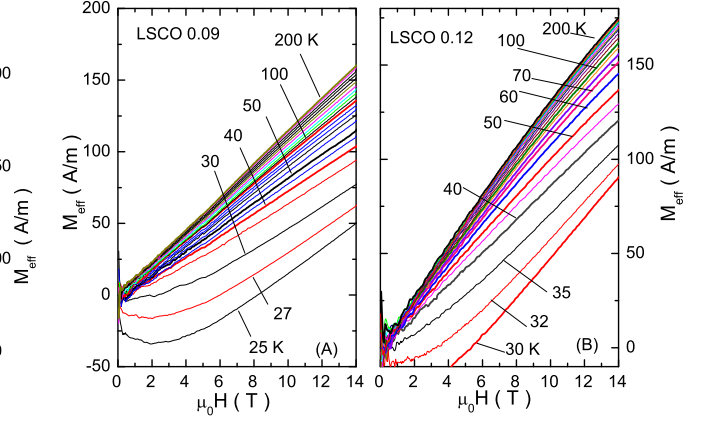
FIG. 9: (color online) Plots of the temperature dependence of $M_{eff}(T)$ in Bi 2201 (Panel A) and in LSCO (B), showing the onset of diamagnetism as T is decreased. In both panels, the value of M_{eff} measured at $H = 14$ T is plotted vs. T in samples with various doping levels x. In general, M_{eff} at high T varies weakly vs. T, as shown by the straight lines which are of the form $A + BT$. Relative to this linear background, M_{eff} shows a strong downwards deviation starting at the onset temperature T_{onset}^M (indicated by arrows).

VI. ONSET TEMPERATURES AND PHASE DIAGRAM

An important question is how high in temperature does the diamagnetic signal extend above T_c. Following the procedure in Wang et al. [10], we have plotted the total effective magnetization M_{eff} measured in fixed H (14 T) versus T. Figure 9 displays these plots for several samples of Bi 2201 (Panel A) and LSCO (Panel B). In agreement with the results for Bi 2212 in Ref. [10], M_{eff} displays a weak T dependence at elevated T that may be fitted to the Van Vleck anisotropy term $\Delta\chi_p = A + BT$ (straight lines). The anisotropy $\Delta\chi_p$ leads to a paramagnetic torque background, as displayed. In each sample, $M_{eff}(T)$ displays a sharp downward deviation, beginning at the temperature defined as T_{onset}^M (arrows). This reflects the appearance of local supercurrents induced in response to the applied field. While feeble near T_{onset}^M, the diamagnetic term $M_d(T)$ grows very rapidly in magnitude to pull M_{eff} to large negative values.

To determine T_{onset}^M with reasonable accuracy, it is important to establish the Van Vleck term χ_p with a sufficiently dense set of points above T_{onset}^M. At elevated temperatures, the magnetization curves become closely spaced. Thus, the stability of the cantilever as well as the resolution in measuring M_{eff} must be sufficiently high to allow adjacent curves to be distinguished. As examples, we display in Fig. 10 A and B expanded views of

the curves in LSCO 09 and LSCO 12, respectively. The values of M_{eff} at $H = 14$ T are the ones plotted in Fig. 9.

The profile of M_{eff} vs. T is common to all the samples investigated, even those in the extreme UD regime. The characteristic profile is qualitatively different from that seen in the gaussian regime in BCS superconductors. Remarkably, the rapid downward acceleration of the diamagnetic signal matches the equally rapid growth of the Nernst signal taken at 14 T (Fig. 3 in Ref. [10] compares the profiles of the Nernst signal and M_d measured in the same crystal of Bi 2212).

To compare T_{onset}^M obtained here with the onset temperature of the vortex Nernst signal T_{onset}^ν [2], we plot the 2 onset temperatures vs. doping x in the phase diagram for LSCO (Fig. 11A) and Bi 2201 (Fig. 11B). Remarkably, in LSCO, T_{onset}^M (open squares) is nominally equal to T_{onset}^ν in LSCO over the entire doping range investigated. The major difference is that the former seems to peak at $x = 0.12$ whereas the latter peaks at 0.10. The error bars at both temperatures are too large to determine if the disagreement is real. In the interesting UD side, both temperatures decrease roughly linearly with x as $x \to 0$. [In an earlier analysis [2], T_{onset}^ν was extrapolated below $x = 0.05$ to reach 0 at $x = 0.03$. Our recent results show that this extrapolation is incorrect. Because the Nernst signal at $x = 0.03$ is too weak to resolve even at low T, there is actually no experimental information on T_{onset}^ν. By contrast, the results on M_{eff} vs. T (Fig. 9B) allow T_{onset}^M to be fixed reliably at small x.] Interestingly, the x dependence of H_{c2} obtained in Ref. [15]
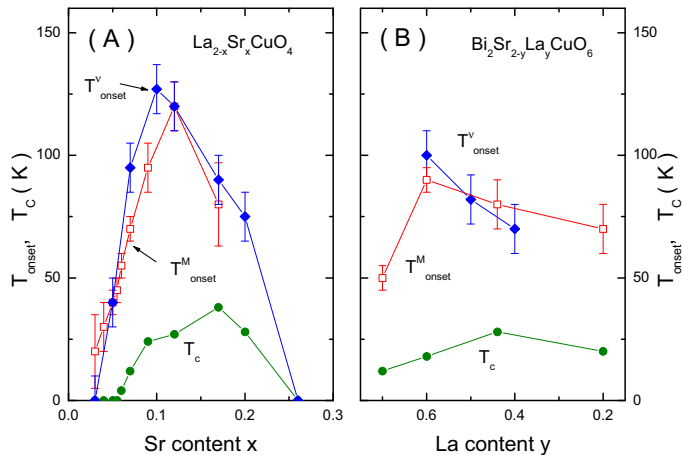
FIG. 11: (color online) Phase diagram comparing the onset temperatures for the Nernst and diamagnetism signals vs. doping x in $La_{2-x}Sr_xCuO_4$ (Panel A) and in $Bi_2Sr_{2-y}La_yCuO_6$ (Panel B). The superconducting transition temperature T_c (solid circles) is plotted with the onset temperature T^ν_{onset} determined by the Nernst effect (solid diamonds), and T^M_{onset} determined by torque magnetometry (open squares). In Panel B for $Bi_2Sr_{2-y}La_yCuO_6$, a large La content y implies small hole carrier concentration (UD regime).

is also linear in x in this regime.

In Bi 2201 (Panel B), the 2 temperature scales are also quite similar. However, the trend of T^ν_{onset} on the OV side appears to be slightly steeper than that of T^M_{onset}. A caveat is that the torque measurements here were not performed on the same crystals as the Nernst experiments.

For the equivalent phase diagram of Bi 2212, see Ref. [10]. The phase diagram for YBCO appears in Ref. [24].

VII. DISCUSSION

Diamagnetism and Supercurrent Response
The presence of a large diamagnetic response that is both strongly T dependent *and* non-linear in H deeply implicates Cooper pairing. Diamagnetism involves an orbital current density $\mathbf{J}$ that is antiparallel to the applied vector potential $\mathbf{A}$ (as in the London equation). Cooper pairing is – to our knowledge – the only established electronic state capable of generating the current response consistent with the nonlinear, strongly T-dependent diamagnetism reported here. [Core diamagnetism in insulators and Landau diamagnetism (observed in pure Bi) are both strictly H-linear to extremely large H ($\mu_B H \simeq W$, where W is the band-width and μ_B the Bohr magneton) and nearly T independent. A "superdiamagnetic" state based on toroidal, orbital moments has been theorized [21], but this state has never been observed.] Hence, diamagnetism provides a rather direct detector of incip-

ient Cooper pairing in the cuprates.

As shown in Secs. III, IV and V for LSCO, the Bi-based cuprates and YBCO, respectively, the M_d-H curves above T_c show similar patterns - a broad minimum in moderate fields followed by a steady suppression to zero in very high fields. This pattern evolves continuously from the curves measured below T_c, which display a divergence at low field caused by the Meissner effect. Above T_c, this divergence vanishes because of the loss of long range phase coherence. Nonetheless, a reduced local phase rigidity survives [11], which gives rise to the enhanced diamagnetic M_d above T_c at low fields. Although its overall magnitude is $\sim$10 times smaller than below T_c (when observed at similar H), M_d is readily detected as a strongly T-dependent and H-nonlinear response. In UD Bi 2201, we have accomplished full field suppression of M_d in fields $\sim$45 T. However, in all other cuprates, the full suppression requires fields in excess of 80 T (possibly as high as 150 T). These impressively large field scales are a consequence of the anomalously large binding energies of Cooper pairs in hole-doped cuprates. The broad similarity of the magnetization curves in LSCO, Bi 2201, Bi 2212 and YBCO suggests that the diamagnetic behavior above T_c is universal in the hole-doped cuprates. They are qualitatively different from the diamagnetic response in low-T_c superconductors.

It is instructive to compare the diamagnetism in cuprates with the fluctuating diamagnetism observed in disordered MgB_2. In a recent experiment, Bernardi *et al.* [22] compared the magnetization of pure MgB_2 ($T_c = 39$ K) with disordered $Mg_{1-x}B_2Al_x$ ($x = 0.25$, $T_c = 25$ K). In the disordered sample (which has a broad transition width of $\sim$15 K), the curves of M_d vs. H show that sizeable diamagnetism exists in the narrow interval 28-32 K above its T_c (Fig. 5 of [22]). The profile of M_d vs. H, which displays a broad minimum at $\sim$ 200 Oe, is roughly similar to the profiles reported here (aside from the field scale). The broad transition width implies large inhomogeneities in the Al distribution. As the diamagnetic response above T_c does not persist above T_c of pure MgB_2 (39 K), we suggest that the fluctuation diamagnetism arises from Al-poor regions of MgB_2 which have the highest T_c. Thus, over the whole sample, diamagnetism is observable above 25 K, but not above 39 K. This contrasts with the cuprates. In the OPT sample within each family, T^M_{onset} extends *above* T_c by factors of 1.3 (YBCO), 1.4 (Bi 2212), 2.1 (LSCO) and 2.5 (Bi 2201). Clearly, we cannot simply explain away the high-T diamagnetism as coming from isolated OPT regions with the highest T_c. The comparison shows that the local supercurrents detected in MgB_2 arise from isolated regions with strong amplitude fluctuations and a broad distribution of local T_c's. By contrast, the diamagnetic signal in cuprates arises from a condensate that has lost phase stiffness, even though the gap amplitude remains large and nominally uniform above T_c.

Quasiparticle term in Nernst signal
In UD LSCO, the quasiparticle (qp) current makes a sig-

nificant contribution to the Nernst signal e_N. In the initial report of Xu *et al.* [1], the onset temperature T_ν was found to remain high even when x falls below 0.1 ($T_\nu \sim 150$ K for $x = 0.05$). This was traced [2] to a significant qp contribution to the Nernst signal. To discuss the qp term, it is crucial to consider the *sign* of the Nernst effect.

By convention, the sign of the Nernst effect is defined as that of the triple product $\mathbf{E}_N \cdot \mathbf{H} \times (-\nabla T)$ with $\mathbf{E}_N$ the observed Nernst E-field [5]. This rule is equivalent to the old convention based on "Amperian" current direction (clearly described by Bridgman [23]). For vortices, $\mathbf{E}_N = \mathbf{B} \times \mathbf{v}_L$ where the vortex line velocity $\mathbf{v}_L$ is $||(-\nabla T)$. Hence vortex flow produces a positive Nernst signal. The qp contribution may have either sign (unrelated to their charge sign).

When the qp term is negative, it is relatively easy to separate the 2 contributions, especially by going to intense H. However, if the qp term is positive, the separation is more difficult. In Ref. [2], Wang *et al.* introduced a method for separating the qp and vortex terms by simultaneous measurements of the Hall angle θ_H and thermopower S vs. H to obtain the term $S \tan\theta_H$. This subtraction procedure yields the onset temperature T^ν_{onset} for the vortex term (45 K at $x = 0.05$), which is plotted in Fig. 11A. With the qp subtraction applied to the samples $x \leq 0.07$, the curve of T^ν_{onset} vs. x has a tilted dome profile with a sharp peak at $x = 0.125$. For OPT and OV LSCO, Wang *et al.* found [5] that the qp term is *negative* and negligible compared with the vortex term. Hence, T^ν_{onset} gives the onset of the vortex term without the need for corrections. (The qp term is also negative in YBCO, Bi 2201 and Bi 2212 [5]).

Recently, this assumption has been challenged by Cyr-Choiniere *et al.* [18], who proposed that rearrangement of the FS – possibly by charge ordering or stripe formation – produces a positive quasi-particle term that dominates the Nernst signal over the LSCO phase diagram at high temperatures. Although their Nernst measurements were largely on Eu-doped and Nd-doped LSCO where static stripes are experimentally observed, they have extended their hypothesis to pure LSCO. There, they proposed that a positive qp also accounts for its Nernst signal at elevated T (except in a narrow interval just above T_c).

In the scenario of Ref. [18], the onset temperature for vortex fluctuations should lie considerably lower than the dome of T^ν_{onset} plotted in Fig. 11A. However, the good agreement between T^M_{onset} and T^ν_{onset} shows that this is not the case. As we argued above, the strongly T- and H-dependent diamagnetism arises only from the pair condensate, and is unaffected by qp contributions. The agreement between T^M_{onset} and T^ν_{onset} seems to us to be strong evidence against the proposal in Ref. [18], at least in pure LSCO. For the claim to be viable, the hypothetical quasiparticles would have to produce a large, T-dependent diamagnetism that is also strongly non-linear in H, as well as a *positive* Nernst signal.

The hypothesis of Cyr-Choiniere *et al.* [18] is the lat-

est of several proposals (see discussion in Ref. [5]) that have sought to explain away the unexpected Nernst signal in the cuprates by invoking quasiparticles with *ad hoc* properties. Are the large Nernst signals at high T from vortices in a phase -disordered condensate or from quasiparticles (qp)? We argue that torque magnetometry and the Nernst effect together constitute an incisive combination that answers this question. When the 2 probes show that a large positive Nernst signal coexists with a diamagnetic susceptibility (with the same onset temperatures and similar profiles vs. T and H), the case in favor of phase slippage in a pair condensate with strongly disordered phase seems compelling to us. This is one of our main conclusions.

The magnetization-Nernst approach can also be turned around to identify situations when the Nernst signal is not caused by vorticity. As mentioned, in UD LSCO ($x < 0.07$) the agreement of T^M_{onset} and T^ν_{onset} provides confirmation that the subtraction proceduce based on $S \tan\theta_H$ [2] is valid. (In the broad interval between T^M_{onset} and T_ν, extending from 45 to 150 K for $x = 0.05$, there is a large positive Nernst signal, but diamagnetism is absent. Thus, even if the qp contribution had not been identified [2], the present experiment would have detected the correct onset of the vortex term.)

In UD $YBa_2Cu_3O_{6+y}$ (YBCO), the qp Nernst signal is unusually large in a narrow window of doping. In this doping range, when the qp term appears at high T, it is negative as in OV LSCO. Significantly, the diamagnetic signal is absent until the vortex Nernst signal appears at a lower T (detailed YBCO results are reported in Ref. [24]). Hence, when used together, the torque magnetization and Nernst effect readily distinguish qp from vortex contributions to the Nernst signal. Nernst effect and diamagnetism studies on $La_{2-x}Ba_xCuO_4$ [20] should provide valuable insight into the fluctuation regime in which stripes coexist with Cooper pairing.

Related Experiments

The surviving pair condensate above T_c has also been observed in other experiments, notably in measurements of the kinetic inductance [25], STM experiments on the gap above T_c [26], and survival of Bogolyubov quasiparticles above T_c [27]. Consistent with these observations, our results imply that the pair condensate exists well above T_c, surviving as a dilute vortex liquid with local phase rigidity of short phase-correlation length. A number of groups recently calculated the Nernst signal and diamagnetism above T_c in 2D superconductors and applied the results to cuprates [28, 29, 30, 31, 32]. The vortex liquid viewed as an incompressible superfluid has been treated by Anderson [33, 34]. A relevant discussion of the relation of the quantum oscillation results to the Nernst and magnetization results is given in Ref. [35].

To summarize, the high-field torque magnetometry measurements reveal that the diamagnetism persists well above T_c in several families of hole-doped cuprates. As a strongly nonlinear M_d vs. H is characteristic of local

supercurrent response, the diamagnetism is direct evidence that the pair condensate exists above T_c, surviving in places all the way to T_{onset}^M. Hence, phase slippage is the origin of the large Nernst effect signals observed to that temperature. The agreement between the onset temperatures T_{onset}^ν and T_{onset}^M precludes quasiparticle interpretations for the positive Nernst signal above T_c. The magnetization results pose very serious difficulties for the quasiparticle hypothesis [18] proposed recently for the Nernst effect in pure LSCO.

[1] Z. Xu, N.P. Ong, Y. Wang, T. Kakeshita and S. Uchida, Nature **406**, 486 (2000).

[2] Yayu Wang, Z. A. Xu, T. Kakeshita, S. Uchida, S. Ono, Yoichi Ando, and N. P. Ong, Phys. Rev. B **64**, 224519 (2001).

[3] Yayu Wang, N. P. Ong, Z.A. Xu, T. Kakeshita, S. Uchida, D. A. Bonn, R. Liang and W. N. Hardy, Phys. Rev. Lett. **88**, 257003 (2002).

[4] Yayu Wang, S. Ono, Y. Onose, G. Gu, Yoichi Ando, Y. Tokura, S. Uchida, and N. P. Ong, Science **299**, 86 (2003).

[5] Yayu Wang, Lu Li, and N. P. Ong, Phys. Rev. B **73**, 024510 (2006).

[6] V. J. Emery, S. A. Kivelson, Nature **374**, 434 (1995).

[7] C. Capan, K. Behnia, J. Hinderer, A. G. M. Jansen, W. Lang, C. Marcenat, C. Marin, and J. Flouquet, Phys. Rev. Lett. **88**, 056601 (2002).

[8] F. Rullier-Albenque, R. Tourbot, H. Alloul, P. Lejay, D. Colson, and A. Forget, Phys. Rev. Lett. **96**, 067002 (2006)

[9] F. Rullier-Albenque, H. Alloul, Cyril Proust, P. Lejay, A. Forget, and D. Colson, Phys. Rev. Lett. **99**, 027003 (2007).

[10] Yayu Wang, Lu Li, M. J. Naughton, G. Gu, S. Uchida and N. P. Ong, Phys. Rev. Lett. **95**, 247002 (2005).

[11] Lu Li, Yayu Wang, M. J. Naughton, S. Ono, Yoichi Ando, and N. P. Ong, Europhys. Lett. **72**, 451 (2005).

[12] Lu Li, Yayu Wang, J.G. Checkelsky, M.J. Naughton, Seiki Komiya, Shimpei Ono, Yoichi Ando, and N.P. Ong, Physica C **460-462**, 49 (2007).

[13] Lu Li, Yayu Wang, M.J. Naughton, Seiki Komiya, Shimpei Ono, Yoichi Ando, N.P. Ong, J. Magnetism Magnetic Mater. **310**, 460 (2007).

[14] N. P. Ong, Yayu Wang, Lu Li, and M. J. Naughton, Phys. Rev. Lett. **98**, 119702 (2007).

[15] Lu Li, J. G. Checkelsky, Seiki Komiya, Yoichi Ando and N. P. Ong, Nature Physics **3**, 311 (2007).

[16] D. C. Johnston, and J. H. Cho, Phys. Rev. B **42**, 8710 (1990).

[17] A. Lascialfari, A. Rigamonti, L. Romano', A.A. Varlamov, and I. Zucca, Phys. Rev. B **68**, 100505(R) (2003).

[18] Olivier Cyr-Choiniere *et al.*, Nature, **458**, 743 (2009).

[19] C. Bergemann, A. W. Tyler, A. P. Mackenzie, J. R. Cooper, S. R. Julian, and D. E. Farrell, Phys. Rev. **B** 57, 14387 (1998).

[20] Q. Li, M. Hučker, G. D. Gu, A. M. Tsvelik, and J. M. Tranquada, Phys. Rev. Lett. **99**, 067001 (2007).

[21] V. L. Ginzburg, A. A. Gorbatsevich, Yu. V. Kopayev and B. A. Volkov, Solid State Commun. **50**, 339 (1984).

[22] E. Bernardi, A. Lascialfari, A. Rigamonti, and L. Romano', Phys. Rev. B **77**, 064502 (2008).

[23] P. W. Bridgman, Phys. Rev. **24**, 644 (1924).

[24] Minhao Liu, Yayu Wang, Lu Li and N. P. Ong, *in preparation*.

[25] J. Corson, R. Mallozzi, J. Orenstein, J. N. Eckstein, and I. Bozovic, Nature, **398**, 221 (1999).

[26] Kenjiro K. Gomes, Abhay N. Pasupathy, Aakash Pushp, Shimpei Ono, Yoichi Ando, Ali Yazdani, Nature, **447**, 569 (2007).

[27] Jhinhwan Lee, K. Fujita, A. R. Schmidt, Chung Koo Kim, H. Eisaki, S. Uchida, and J.C. Davis, Science **325**, 1099 (2009).

[28] L. Benfatto, C. Castellani, T. Giamarchi, Phys. Rev. Lett. **98** 117008 (2007); *ibid.*, Phys. Rev. Lett. **99**, 207002 (2009).

[29] V. Oganesyan, D. A. Huse, and S. L. Sondhi, Phys. Rev. B, **73**, 094508 (2006).

[30] Z. Tešanović, Nature Physics **5**, 408 (2008).

[31] Daniel Podolsky, Srinivas Raghu, and Ashvin Vishwanath, Phys. Rev. Lett. **99**, 117004 (2007).

[32] Subroto Mukerjee and David A. Huse, Phys. Rev. B **70**, 014506 (2004).

[33] P. W. Anderson, Nature Physics **3**, 160 (2007).

[34] P. W. Anderson, Phys. Rev. Lett. **100**, 215301 (2008).

[35] T. Senthil, P. A. Lee, Phys. Rev. B **79**, 245116 (2009).